Journal of Molecular Liquids 165 (2012) 119–124

Contents lists available at SciVerse ScienceDirect

Journal of Molecular Liquids

journal homepage: www.elsevier.com/locate/molliq

Interaction study of ss-DNA and Yb^{3+} ions in aqueous solutions by electrochemical and spectroscopic techniques

Hoda Ilkhani [a,b], Mohammad Reza Ganjali [b,c,*], Majid Arvand [a], Parviz Norouzi [b,c]

[a] Department of Chemistry, Faculty of Science, University of Guilan, P.O. Box 1914, Rasht, Iran
[b] Center of Excellence in Electrochemistry, Faculty of Chemistry, University of Tehran, Tehran, Iran
[c] Endocrinology & Metabolism Research Center, Tehran University of Medical Sciences, Tehran, Iran

ARTICLE INFO

Article history:
Received 12 September 2011
Received in revised form 20 October 2011
Accepted 28 October 2011
Available online 19 November 2011

Keywords:
Ytterbium
DNA
Voltammetry
Spectroscopy
Computational study

ABSTRACT

In this work, for the first time the electrochemical behavior of the Yb^{3+} and Yb^{3+} ion interactions with short single strand DNA (ssDNA) sequence at two pHs was studied. Then the UV–vis spectroscopic method was used for supporting these pieces of evidence. The interaction between Yb^{3+} and ssDNA has different binding modes at different pHs. The ratio between [Yb^{3+}] and [ssDNA] is dependent to pH and pK_a of DNA bases. In pH 3.7, Yb^{3+} binds to ssDNA mainly by electrostatic attraction. Binding number, n, of 2 of Yb^{3+} per ssDNA and binding constant were obtained with Cyclic Voltammetry (CV) and differential pulse voltammetry (DPV) methods, respectively. In this pH, the bases of ssDNA are totally protonated and Yb^{3+} interacts electrostatically with phosphate groups. The UV–vis study showed similar results. The results at pH 5.5 show that Yb^{3+} can bind to ssDNA with electrostatic and covalent bonds. In this pH, besides phosphate groups, the bases can be interacted to Yb^{3+}, too. The binding number 4 of Yb^{3+} per ssDNA was obtained. Computational studies were done and confirmed the result of experimental data. The agreement mutually verifies the accuracy of the methods.

1. Introduction

The diverse nature of medical applications of lanthanides may come as a surprise to many researchers. Recently lanthanides have attracted researcher interests, primarily as a gadolinium-based MRI contrast agents, as hypophosphatemic agents for kidney dialysis patients, as luminescent probes in cell studies, and for palliation of bone pain in osteosarcoma [1].

The biological properties of the lanthanides are similar to calcium and they have stimulated research into their therapeutic application. The lanthanides have similar ionic radii to calcium, but by virtue of possessing higher charge densities, they have a high affinity for Ca^{2+} sites on biological molecules [2].

The knowledge of the DNA structure and its interactions with other compounds can lead to advances in pharmacology and diagnosis basis of many diseases [3–7].

Nucleic acids are responsible for the storage and transcription of genetic information in living cells and are involved in protein synthesis. Nucleic acids are polymers of nucleoside phosphates and hence negatively charged in neutral solutions. Then they interact strongly with metal ions. These interactions are important in nature, because it will change the genetic material's structure and function [8]. The interaction of DNA with heavy metals, since they are involved in processes leading to DNA damage, has been extensively investigated [9].

The study of the metal–DNA interactions becomes uniquely important to understand the consequent conductive behavior and its electron transfer property. The evidence for the binding of metal ions to DNA is rather indirect and still remains a matter of discussion [10].

DNA is a negatively charged polyelectrolyte, and the binding of metal cations to it, is of importance since this plays a crucial role in the biological activity of nucleotides and nucleic acids, changing their properties in ways that depend on the nature of the metal ion. Knowledge of the mechanisms responsible for the activity of these systems requires the study of metal ion–nucleic acid interactions [11].

Among the lanthanide series, just five members are electroactive. Ytterbium is one of them. The other ones are cerium, europium, samarium, and terbium.

The interaction of these metal ions with DNA was studied by several methods such as luminescent [10,12], UV–vis spectroscopy [13], NMR [14,15] and electrochemistry [16–18] but the interaction of lanthanides with a short single strand DNA sequence by electrochemical method wasn't studied.

Also in recent years, computational methods are applied in different branches of chemistry. In the presented paper, we have also used B3LYP/SBKJC method to study the interaction [19].

In this paper, the electrochemical behavior of Yb^{3+} has been studied by Cyclic Voltammetry (CV) and differential pulse voltammetry (DPV)

* Corresponding author at: Center of Excellence in Electrochemistry, Faculty of Chemistry, University of Tehran, Tehran, Iran. Tel.: +98 21 61112788; fax: +98 21 66405141.
E-mail address: ganjali@khayam.ut.ac.ir (M.R. Ganjali).

0167-7322/$ – see front matter © 2011 Elsevier B.V. All rights reserved.
doi:10.1016/j.molliq.2011.10.017

for the first time. Then the interaction between ssDNA with Yb^{3+} has been studied at two pHs and with two methods: UV–vis spectroscopy and electrochemistry. The experimental results have proved that Yb^{3+} could interact with ssDNA mainly by electrostatic binding and by binding number, n, 1, but in higher pH, the interaction between Yb^{3+} and ssDNA is not only electrostatic but also covalent binding and the binding number is higher.

2. Experimental

2.1. Apparatuses

Electrochemical experiments were performed using AUTO LAB PGSTAT 30 electrochemical analysis system and general propose electrochemical system (GPES) 4.9005 software package (Eco Chemie, The Netherlands). A PERKIN-ELMER UV–vis spectrophotometer with a 1 cm path cell was used for spectrophotometric determinations. Also a Heidaloh MR 3001K stirrer was used in this work.

2.2. Reagents

A 10-mer oligonucleotide was supplied (as lyophilized powder) from MWG-Biotech AG, with the following sequence: 3′-GGAGCTCCTG-5′. The stock solutions of short ssDNA sequence (1.0×10^{-2} M) were prepared by dissolving powder primer in doubly distilled water and kept frozen in −20 °C temperature.

Yb_2O_3 was obtained from Merck Co. The stock solution of Yb^{3+} (1×10^{-2} M) was prepared by dissolving 0.366 g of its oxide in minimum amount of nitric acid and diluted with phosphate buffer (pH 3.7 and 5.5) in 100 mL volumetric flaks. Dilute solution was prepared just before use.

2.3. Electrochemical studies

Cyclic Voltammetry (CV) experiments were carried out at room temperature (23 ± 2 °C) in a potential ranging from −0.7 V to 0.0 V at various scan rates (from 5 mV s^{-1} to 300 mV s^{-1}). Only reproducible responses were recorded.

For differential pulse voltammetry (DPV), the conditions were as follows: the step potential 0.01 V, the modulation time 0.04 s, and the interval time 0.53 s, in a potential range from −0.65 V to −0.2 V.

All voltammetric experiments were performed in a single compartment glass cell of three electrode assemblies of 500 μL capacity in which platinum wire was used as counter electrode, Ag/AgCl was used as the reference electrode and platinum electrode was used as working electrode. Prior to each electrochemical experiment, the working electrode was polished successively with 0.3 μm (grain size) alumina powder (Metrohm) and then cleaned ultrasonically in water.

Interaction between ssDNA and Yb^{3+} was carried out in constant concentration of Yb^{3+} and varying concentrations of ssDNA by CV and DPV methods. Vice versa, for UV–vis titration of ssDNA with Yb^{3+}, the concentration of ssDNA was kept constant and various concentrations of Yb^{3+}, were added, up to 3 mL final volume.

2.4. Computational methods

Calculations on the isolated ssDNA and Yb^{3+}–ssDNA were performed within Gamess package [20].

Each species was initially optimized with PM3 method and, then the optimized structures were again optimized with B3LYP/SBKJC. Full geometry optimizations and frequency calculations were performed and each species was found to be minima by having no negative values in the frequency calculation. The calculations gave internal energies at 0 K. In order to obtain gas phase free energies at 298.15 K, it is necessary to calculate the zero-point energies and thermal corrections together with entropies to convert the internal energies to Gibbs energies at 298.15 K [21].

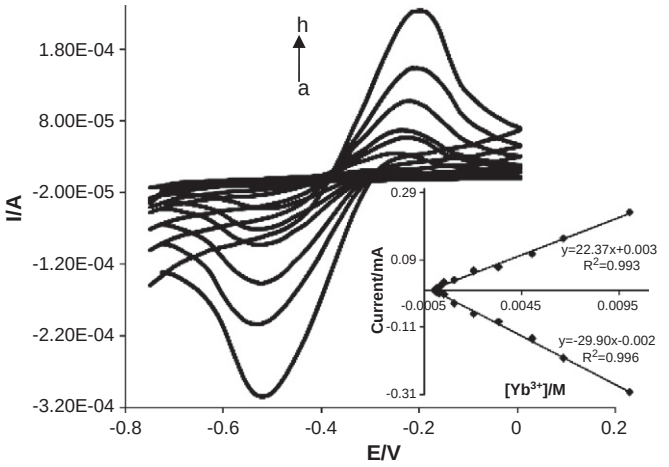

Fig. 1. CVs of Yb^{3+} in 0.1 M NaCl at pH 3.7 and potential range −0.5 V to −0.25 V. Yb^{3+} concentrations were: (a) 2.5×10^{-4} M, (b) 5.0×10^{-4} M, (c) 1.0×10^{-3} M, (d) 2.0×10^{-3} M, (e) 3.33×10^{-3} M, (f) 5.0×10^{-3} M, (g) 6.6×10^{-3} M, and (h) 1.0×10^{-2} M. The scan rate was 0.1 V s^{-1}. Inset: Plot of I_p vs. concentration of Yb^{3+} at the same conditions.

3. Results and discussion

3.1. Electrochemical study

3.1.1. Electrochemical behavior of Yb^{3+}

The CVs for the ytterbium (III) nitrate phosphate buffer (pH 3.7) are shown in Fig. 1. Forward scans reveal that the anodic peak associated with the oxidation of Yb^{3+} to Yb^{4+} occurs at approximately −212.8 mV. On the reverse scan, the cathodic peak associated with reduction of Yb^{4+} to Yb^{3+} occurs at approximately −530.2 mV versus Ag/AgCl. Fig. 1 shows the CVs of Yb^{3+} in different concentrations too. The concentration of Yb^{3+} ranged from 2.5×10^{-4} M to 1.0×10^{-2} M as can be seen in this figure, there are pair of redox peaks for Yb^{3+}. Anodic and cathodic peak currents changed slightly with increasing concentration. Also the peak potential is constant with increasing the concentration of Yb^{3+} ion and I_{pc}/I_{pa} is very near to one. Thus, this result shows that the redox peak is reversible. Inset of this figure shows that the relationship between I_p and concentration of Yb^{3+}, is linear.

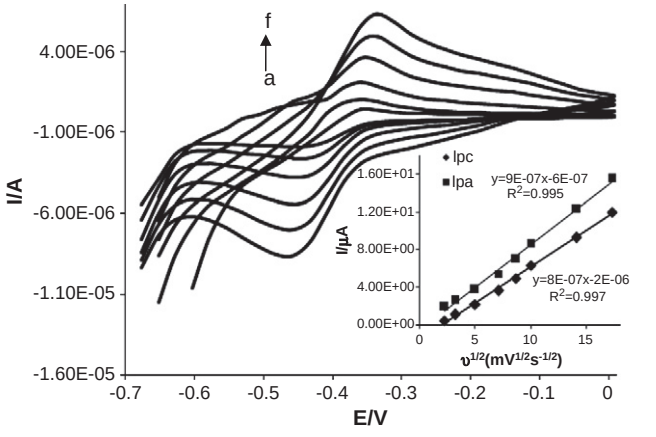

Fig. 2. CVs of 5.0×10^{-4} M Yb^{3+} in 0.1 M NaCl at pH 3.7 and potential range −0.7 V to −0.1 V. Scan rates are (a) 5 mV s^{-1}, (b) 10 mV s^{-1}, (c) 50 mV s^{-1}, (d) 100 mV s^{-1}, (e) 200 mV s^{-1}, and (f) 300 mV s^{-1}. Inset: Plot of I_p vs. square root of scan rates at the same conditions.